Foam Assisted Cyclic Solvent Injection in Heterogeneous Reservoirs

Sahand Etemad [1,2], Jihua Dong [2], Apostolos Kantzas [1,2]*

[1]Department of Chemical and Petroleum Engineering, University of Calgary, Calgary, AB, Canada
[2]PERM Inc. TIPM Laboratory, Calgary, AB, Canada

Abstract. In the unconsolidated heavy oil resources of the Lloydminster area, located on the Alberta and Saskatchewan border, Cold Heavy Oil Production with Sand (CHOPS) is the primary production process. However, 85 to 95% of the Original Oil in Place (OOIP) is left behind in many post-CHOPS reservoirs. The objective of this research is to apply subsequent enhanced oil recovery techniques in post-CHOPS reservoirs to produce additional oil. We evaluated oil recovery and CO_2 storage enhancement with and without pre-injecting a slug of foam prior to the solvent flood in heterogeneous reservoirs. We investigated the effects of adding biodegradable Cellulose Nanocrystals (CNC) to foam to block highly permeable wormholes induced during the sand production stage in CHOPS operations. Eight heterogeneous sandpacks with highly permeable wormholes in the centre were then created to mimic post-CHOPS reservoirs. Cyclic Solvent Injection (CSI) and Foam-CSI cycles were run, and it was observed that the addition of foam can plug the highly permeable zones and increase oil recovery by up to 14%OOIP. Solvent flowed into the matrix during CSI after the foam flood. Consequently, in the production stage, a higher volume of solvent-diluted oil was produced. The proposed technology can offer significant commercial potential in post-CHOPS reservoirs.

1 Introduction

The Lloydminster area is located in east-central Alberta and west-central Saskatchewan. It contains bitumen and heavy oil-saturated oil sands. It is estimated that there are 50 to 70 billion barrels of oil in place in these reservoirs [1]. Due to factors such as high oil viscosity, low Gas-Oil Ratio (GOR), and initial reservoir pressures, primary recovery methods have shown low efficiency for these formations.

Oil resources in the Lloydminster area are primarily extracted using Cold Heavy Oil Production with Sand (CHOPS). CHOPS is a non-thermal recovery method that involves the production of heavy oil along with sand [2]. In this primary recovery technique, sand influx continues throughout the production life of the well. The primary recovery mechanisms in CHOPS are the presence of foamy oil and wormholes, which are highly permeable zones introduced during sand withdrawal in CHOPS reservoirs. Under CHOPS, typical recovery factors are between 5 to 15% of the Original Oil in Place (OOIP) [2, 3]. This means that around 90% of the oil remains untapped in the ground, making CHOPS fields ideal candidates for Enhanced Oil Recovery (EOR) methods.

It is believed that following CHOPS production, the reservoir is left with a system of highly permeable channels [4]. Because the system of wormholes provides the path of least resistance for the injected fluids, it makes the depleted CHOPS reservoirs unsuitable for conventional flooding processes. Since CHOPS reservoirs typically have small net pays, usually less than 10 meters, solvent-based methods are better in post-CHOPS reservoirs than steam-based techniques due to significant heat loss in thermal recovery methods [5, 6]. Various solvent-based methods, such as solvent injection [7], Vapor Extraction (VAPEX) [8], Solvent Vapor Extraction (SVX) [9], and Cyclic Solvent Injection (CSI) [10], have been suggested for post-CHOPS reservoirs in the literature. In the CSI process, the presence of wormholes can increase the contact surface area between the solvent and heavy oil. Additionally, these wormholes provide flow channels through which solvent-diluted oil can flow back to the wellbore. Consequently, the CSI process is more promising as a post-CHOPS enhanced heavy oil recovery method compared to VAPEX and SVX processes [11].

During CSI, solvent is injected into a well to dilute the heavy oil. The well is shut in to soak for a period, allowing the injected solvent time to dissolve into the heavy oil. Then, the same well is opened, and the solvent-diluted heavy oil with lower viscosity is produced [12]. The CSI process is repeated in many cycles until the oil cut in the production becomes too small. Figure 1 shows a schematic of a cyclic solvent injection process for heavy oil recovery.

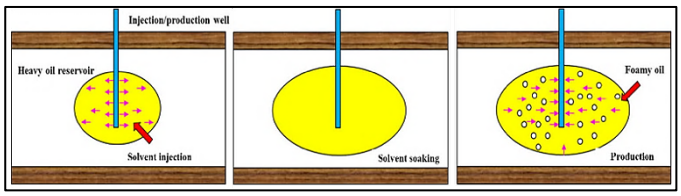

Fig. 1. Solvent injection inside the reservoir (Left), soaking time for the solvent to dissolve inside the oil (Middle), and production stage with foamy oil flow (Right), adapted from [13].

* Corresponding author: sahand.etemad@ucalgary.ca

There have been limited studies conducted in the literature to explore the CSI process as a follow-up technique for post-CHOPS reservoirs. [14] conducted an experimental study to assess the efficiency of a ″28% C_3H_8 - 72% CO_2″ solvent mixture in a CSI process post-CHOPS. They conducted six cycles and achieved a recovery factor of 50%. Soaking periods during CSI were as long as 62 days during their tests. A study was conducted by [15] using a cyclic CO_2 injection experiment to assess the feasibility of using CO_2 to recover additional oil from post-CHOPS reservoirs. Their findings suggest the potential for repressurizing depleted heavy oil reservoirs through CO_2 injection, particularly for those reservoirs that had low recovery factors during primary depletion. [16] investigated the effects of injection pressure, soaking time, and solvent composition on cyclic solvent injection experiments. Experiments were conducted in a Berea sandstone core.

In post-CHOPS reservoirs, a key feature is the presence of wormholes. Previous studies did not account for the effects of these highly permeable layers on the CSI efficiency. In recent years, new research has been carried out to explore methods for enhancing the performance of the CSI process in the presence of wormholes. [17] performed a hybrid cyclic solvent injection, along with chasing hot water injection as the solvent retrieval agent, in a post-CHOPS medium with wormholes. Their findings indicated that the process efficiency is influenced by the patterns of the wormhole network, with a subsequent hot water flush contributing positively to solvent retrieval. [18] proposed combined cyclic CO_2 injection and waterflooding (WF-CSI) as a follow-up technique to recover additional heavy oil from post-CHOPS reservoirs in the presence of wormholes. [19] proposed Gas Flooding-Assisted CSI (GA-CSI) to improve the effectiveness of the CSI process. In this approach, a gas slug was injected following the pressure depletion phase to generate partially diluted foamy oil within the solvent chamber. The results demonstrated that GA-CSI has the potential to increase the oil production rate by more than threefold compared to conventional CSI process.

Foam-Assisted Cyclic Solvent Injection (FA-CSI) has emerged as a potential solution to improve recovery rates in post-CHOPS reservoirs with wormholes. Foams can improve the solvent flood during CSI through mobility control by restricting the flow in highly permeable wormholes and hinder solvent channeling. The subsequent solvent will flow through the low-permeable layers containing oil. [20] investigated the performance of a surfactant foam over a large range of drawdown rates in cores; faster drawdown rates resulted in higher oil recovery. Additionally, they showed that high residual oil saturations are detrimental to foam formation. [21] demonstrated that foam-assisted chemical flooding was able to increase the ultimate oil recovery by 5% of OOIP after water flooding, and injection of pre-generated foam increased ultimate oil recovery by 13% of OOIP after water flooding compared to in situ foam generation.

This paper presents an experimental study to evaluate the efficiency of FA-CSI for enhanced heavy oil recovery in post-CHOPS reservoirs with wormholes. We are investigating the effects of adding biodegradable and wood-derived Cellulose Nanocrystals (CNC) to a surfactant-based foam on mobility control and oil recovery in a post-CHOPS reservoir. We hypothesize that the CNC foams will block the higher permeable zones induced during primary CHOPS and improve the subsequent solvent flood. Additionally, we are exploring the enhancement of CO_2-based CSI by adding propane to the CO_2 stream. Our goal is to maximize CO_2 injection with minimal back-production. We evaluate oil recovery and CO_2 storage enhancement with and without the pre-injection of a slug of foam prior to production.

2 Materials and Methods

2.1 Porous media

Sandpacks containing wormholes were utilized in the laboratory to simulate the geological formations in post-CHOPS reservoirs. These packs are formed by compacting sand into a cylindrical tube to create pore spaces. Wormholes are artificially introduced channels within the sandpack that mimic high-permeability pathways, similar to those created by sand production during CHOPS. These wormholes can increase fluid flow through the pack. To create these sandpacks, two sets of homogeneous sand mixtures, coarse for wormholes and fine for the matrix, were dry-packed into a shrinking tube and a cylindrical tube with a smaller diameter located in the center of the main shrinking tube (imagine a tube within a tube). After simultaneous packing to a length of 1 ft and tapping on the shrinking tube for compaction, the smaller diameter tube in the center was slowly pulled out. Eight sandpacks with centered wormholes were created by dry packing to simulate post-CHOPS reservoirs. The properties of the sands, matrix, and wormhole are shown in Figure 2 and Table 1. Different sizes of Lane Mountain silica sands were used to pack both the matrix and wormhole simultaneously. Table 1 illustrates the size range and permeability to gas for two types of sands used for packing the sandpacks. The permeability ratio of the wormhole to the matrix was two. Wormholes were centered, and two different diameters were created to evaluate their effects on CSI and FA-CSI floods. Eight different sandpacks with wormhole diameters of 0.5″ and 1″ were packed with the following properties: Porosity (%): 37.1 ± 0.5, Kg (D): 5.7 ± 0.6, Swi (%): 0.1 ± 0.02, PV (cc): 514 ± 17.

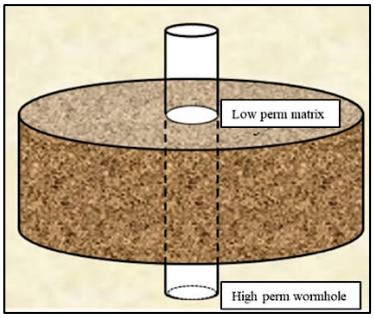

Fig. 2. 3D cross sectional view of a sandpack with a centered wormhole.

Table 1. Properties of the sands used to pack both the matrix and wormhole.

	Sand size, µm	Kg (D)
Wormhole	177-297	9.17
Matrix	149-177	4.60

2.2 Chemicals and oil

We blended different viscose oils to achieve a viscosity of 16000 mPa·s for the oil, within the range of oil viscosities found in the Lloydminster formation, and then measured the density, viscosity and water cut values. Synthetic and crude oils with different viscosities were mixed. Please refer to Table 2 for the types of oils used in the blending stage.

Table 2. Oil types and their viscosities.

Oil type	Viscosity, cp
Oilfield 1	3982
Oilfield 2	2.00E+04
Oilfield 3	3.50E+04
Oilfield 4	5.30E+04
Oilfield 5	7.20E+04
Oilfield 6	8.00E+04
Oilfield 7	4.10E+04
White synthetic oil	87

The average oil viscosity value was 16726 mPa·s, oil density was 0.960 g/cc, and water content was 2.6%. All the oil properties measurements were conducted at 20 °C. The solvent mixture for injection during CSI cycles consisted of 0.7 mole fraction CO_2 and 0.3 mole fraction propane. Based on the isobar phase diagrams of the CO_2/C_3H_8 mixture, at a testing pressure of 3400 kPa and a temperature of 20 °C, the solvent was in the gas phase and close to the two-phase region. During the foam flood in the FA-CSI cycles, the foam had a 90% quality, and the gas phase was nitrogen. The foaming solution was made of 1 wt% CNC nanoparticles and 0.1 wt% cationic surfactant, DTAB. Foam stability in the presence and absence of oil and brine under HPHT testing conditions has been extensively discussed in our previous work using the same foaming solution system [22, 23, 24]. During the flooding experiments and for all the tests, the solvent and foam were injected from the production end, with the injection end always closed.

2.3 Core flood apparatus

The schematic of the FA-CSI rig is depicted in Figure 3. Up to five separate sandpack floods were run simultaneously. The rigs consisted of wormhole-induced sandpacks connected to water-saturated vessels at the bottom, to mimic the presence of active aquifers. The schematic of the core flood rig shown in Figure 3 consists of the CSI and foam flood setups, as well as the sampling unit. Foam was pre-generated inside a foamer by co-injecting nitrogen and the foaming solution, 1wt% CNC + 0.1wt% DTAB, prior to the injection inside the sandpacks.

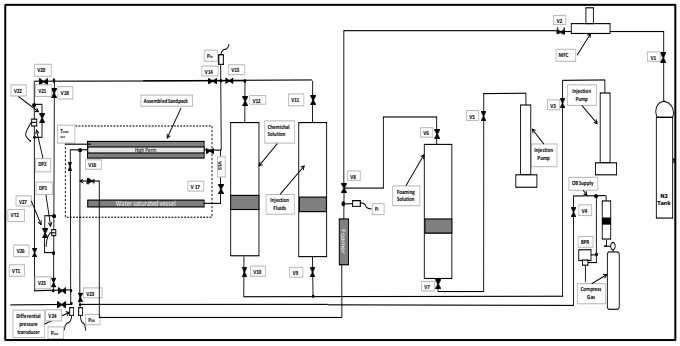

Fig. 3. Schematic of the setup for the CSI and FA-CSI experiments.

The rigs are composed of foam flood and solvent flood setups. The foam flood setup comprises a nitrogen tank, a mass flow controller by Bronkhorst, a foam generator (a 5cm long stainless steel ¼" tubing filled with sand to generate foam through mechanical shear), a Teledyne ISCO liquid pump Model 500D, and a transfer vessel containing the foaming solution, which will be co-injected into the foamer along with N_2. The solvent flood setup consists of transfer vessels containing injected solvent and horizontal sandpacks with centered wormholes, which are connected to a water vessel acting as an aquifer for the reservoir. The locations of the Omega pressure transducers, Validyne differential pressure transducers, and Swagelok valves are shown in the schematic in Figure 3. After packing the sandpacks and vacuuming the air from the porous media, brine and oil injections were carried out. The detailed properties of all eight sandpacks are shown in Table 3.

Table 3. Sandpacks properties.

Core	φ (%)	KB(D)	Ko (D)	Swi (%)	So (%)	PV (cc)
1	37.77	7.19	13.43	0.17	0.83	547.54
2	37.89	7.21	11.66	0.16	0.84	558.43
3	38.18	7.49	14.16	0.15	0.85	471.69
4	36.05	4.31	6.65	0.11	0.89	502.38
5	36.01	4.49	6.88	0.09	0.91	541.8
6	38.00	5.18	7.58	0.07	0.93	468.65
7	35.91	4.78	4.37	0.04	0.96	499.15
8	36.87	5.35	2.06	0.06	0.94	521.19

The flooding procedure for each oil-saturated sandpack was as follows:

1. The first step was primary depletion. At a constant temperature of 20 °C, the pore pressure of the system decreased from 3400 kPa to 200 kPa with a depletion rate of 50 kPa/hr.

2. During the 1st CSI, solvent was injected into the sandpack at 3400 kPa pore pressure. The injection valve

was then closed to allow the solvent and oil to soak for approximately 300 hours. Subsequently, the injection valve was opened for production at a rate of 50 kPa/hr. The CSI cycle was repeated two more times.

3. For the first foam flood, foam was injected at the end of the 3rd CSI until the system pressure reached 2000 kPa. This was followed by the 4th CSI cycle, which consisted of solvent injection at 3400 kPa, soaking time, and then production until the pore pressure reached 200 kPa.

4. The 5th CSI consisted of solvent injection at 2000 kPa pore pressure, followed by a soaking period. After that, foam was injected to reach a system pressure of 3400 kPa. Production started immediately at a rate of 50 kPa/hr after the foam flood.

5. The last step was performing the 6th CSI cycle and 3rd foam flood. Solvent was injected at 2000 kPa pore pressure into the sandpack, and then the system was shut in for soaking to allow the injected solvent time to dissolve into the heavy oil. After that, a third slug of foam was injected to reach a system pressure of 3400 kPa, followed by final depletion at a rate of 50 kPa/hr for the system to return to atmospheric conditions.

3 Results

In this section, a summary of the conducted experiments during primary pressure depletion, CSI, and FA-CSI is presented. Results are interpreted and discussed in terms of pressure drops, production and injection volumes, and recovery factors. For sandpack number 2, all the experiments from the beginning of primary depletion until the end of the 3rd FA-CSI cycle are discussed.

3.1 Primary production

During primary depletion, pressures at both ends of the sandpack were measured, with Pin and Pout shown in Figure 4 with solid and dashed black lines, respectively. Throughout depletion, the total production volume was monitored, as depicted by the red line in Figure 4. Pressure build-up across the sandpack was measured using a Validyne P55 differential pressure transducer. The pressure drops across the sandpack initially increased to 20 kPa, followed by a plateau region. The system's pore pressure reduced from 3400 kPa to 200 kPa with a depletion rate of 50 kPa/hr. The cumulative oil produced during the primary pressure depletion stage was 26.10 g. Considering the OOIP of 443.70 g for sandpack number 2, the RF for the primary production post-CHOPS was 5.88 %OOIP.

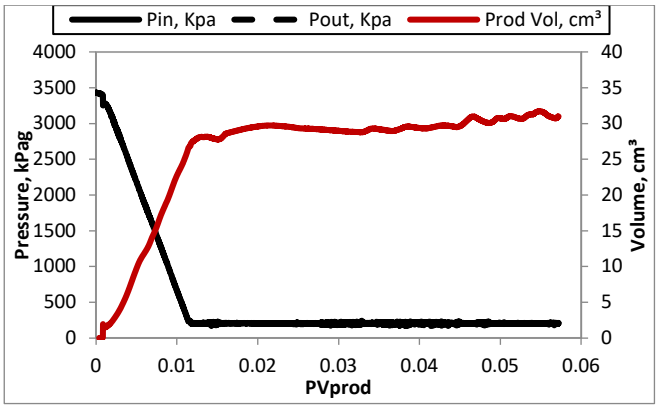

Fig. 4. Inlet and outlet pressures (kPag) and cumulative production volumes (cm^3) during the primary depletion stage.

3.2 1st CSI

During the 1st CSI, after injecting solvent at 3400 kPa pore pressure, a soaking period was undertaken for the solvent to dissolve into the oil, see Figure 5. Cumulative gas production at the end of the soaking time is shown in the red line. The production volume initially increased, then plateaued when the pore pressure reached 200 kPa. The produced water and oil after reaching 200 kPa pore pressure were small enough to terminate the 1st CSI cycle. The final pore pressure before the start of the 2nd CSI was 200 kPa. The total produced oil during the 1st CSI was 61.03 g, with an incremental RF of 13.75 %OOIP.

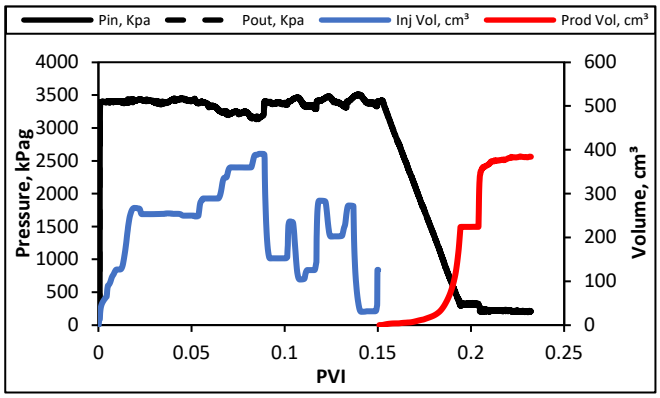

Fig. 5. Inlet and outlet pressures (kPag) and cumulative production and injection volumes (cm^3) during the 1st CSI.

3.3 2nd CSI and 3rd CSI

The results of the 2nd and 3rd CSI cycles are shown in Figures 6 and 7, respectively. By comparing the blue lines in Figures 6 and 7, it is evident that the solvent injection volume increased during the 3rd CSI compared to the 2nd CSI. This increase could be attributed to the availability of more pore space for the solvent in the 3rd CSI cycle after oil production in the 2nd CSI. In both cycles, cumulative production volumes, red lines, initially increased, followed by a long plateau region. Inlet and outlet pressures for the sandpack number 2 were measured and are shown in solid and dashed

black lines in Figures 6 and 7. The produced oil during the 2nd and 3rd CSI cycles was 30.02 g and 22.16 g, respectively, indicating significantly more oil recovery during the 2nd CSI. This higher recovery in the 2nd CSI compared to the 3rd CSI can be attributed to the higher oil in place during this cycle. Incremental oil recovery for all the CSI and FA-CSI cycles will be discussed at the end of Section 3.7.

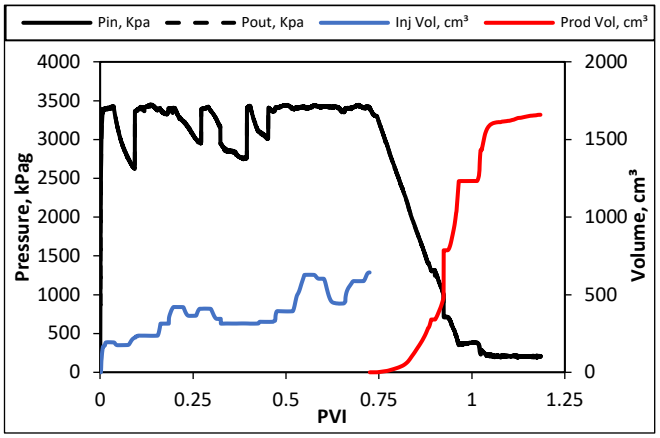

Fig. 6. Inlet and outlet pressures (kPag) and cumulative production and injection volumes (cm³) during the 2nd CSI.

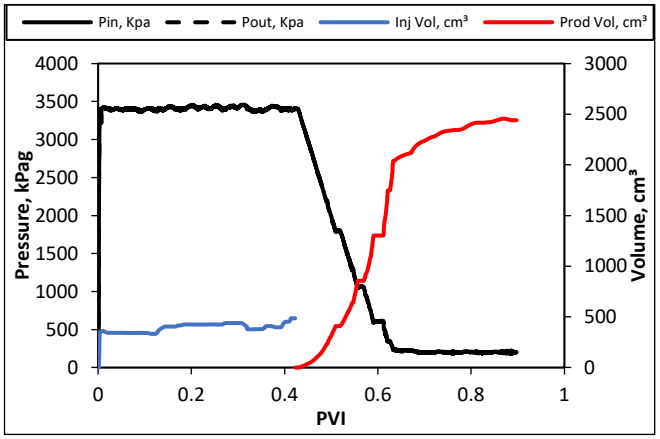

Fig. 7. Inlet and outlet pressures (kPag) and cumulative production and injection volumes (cm³) during the 3rd CSI.

3.4 1st FA-CSI

After the production stage of the 3rd CSI, the 1st FA-CSI started. Solvent was injected from the production end into the sandpack until the system pore pressure reached 2000 kPa. The injected solvent volume is depicted by the blue line in Figure 8. The volume of injected solvent decreased compared to the 2nd and 3rd CSI cycles due to the lower injection pressure as indicated. Following the solvent flood and soaking time, foam injection was conducted until reaching a pore pressure of 3400 kPa in the sandpack, as indicated by a sharp increase in pressure shown by the black line in Figure 8. Figure 9 displays the injected foaming solution volume in the green line, around 17 cc, and the pressure at the inlet and outlet of the sandpack during the foam injection in solid and dashed black lines, respectively. Immediately after foam injection, the production stage of the 1st FA-CSI began. Initially, the production volume increased and then reached a plateau region, as shown by the red line in Figure 8. During production, the pore pressure decreased at a depletion rate of 50 kPa/hr, and the pressure at the end of the 1st FA-CSI reached 200 kPa. Incremental and cumulative production volumes were measured. A higher amount of oil was produced in the early stage of production. The amount of produced oil at the 200 kPa pore pressure was negligible.

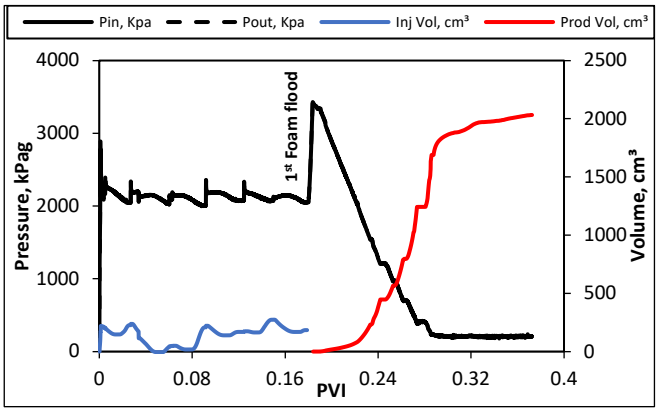

Fig. 8. Inlet and outlet pressures (kPag) and cumulative production and injection volumes (cm³) during the 1st FA-CSI.

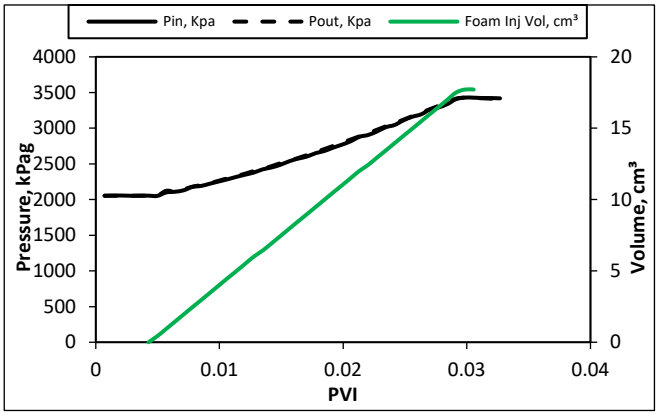

Fig. 9. Foaming solution volume (mL) and Pressure build-ups across the sandpack (kPag) during the 1st foam flood.

A higher amount of water was produced during the production stage of the 1st FA-CSI compared to the previous CSI cycles, which can be attributed to the production of the water-based foaming solution injected before the start of the production. The produced oil at the end of the 1st FA-CSI was 11.54 g, with an incremental RF of 2.6 %OOIP for this stage of the experiments.

3.5 2nd FA-CSI

After the production stage of the 1st FA-CSI, the 5th CSI cycle started, followed by the 2nd slug of foam injection, as depicted by a spike in pressure, see black line in Figure 10. After solvent injection at 2000 kPa pressure and soaking, and before the production stage, around 14 mL of foaming solution was co-injected with nitrogen gas into the reservoir.

Foam flood, followed by solvent flood, allowed for the mitigation of foam-degrading factors, including residence time and solvent destructive effects on lamella. A slug of foam was injected to reach a system pressure of 3400 kPa. After foam injection, the production valve was immediately opened at a depletion rate of 50 kPa/hr, as shown in Figure 10. Production volume was monitored during the depletion stage in the red line. Figure 11 shows the Pin and Pout across the sandpack during the foam injection and the volume of foaming solution injected during the 2nd Foam flood. Cumulative produced oil during the 2nd FA-CSI was 19.59 g, with an incremental RF of 4.4 %OOIP.

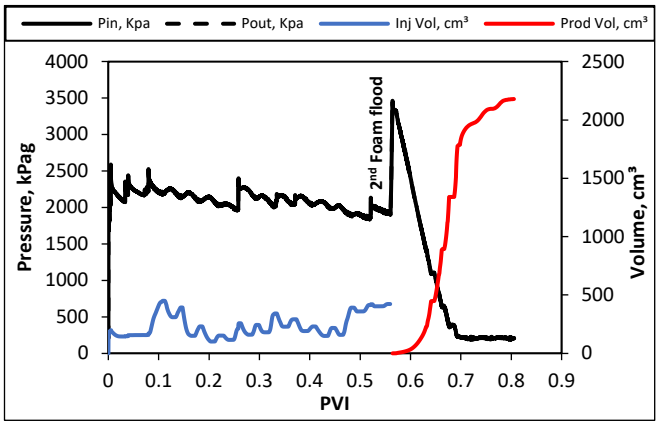

Fig. 10. Inlet and outlet pressures (kPag) and cumulative production and injection volumes (cm^3) during the 2nd FA-CSI.

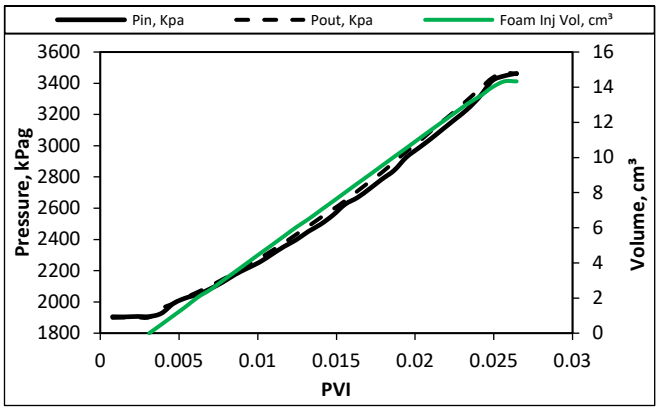

Fig. 11. Foaming solution volume (mL) and Pressure build-ups across the sandpack (kPag) during the 2nd foam flood

3.6 3rd FA-CSI

At the end of the 2nd FA-CSI, solvent mixture was injected into the sandpack at a pore pressure of 2000 kPa. After the soaking period, 12 mL of foaming solution was co-injected into the sandpack with nitrogen gas to reach the target pore pressure of 3400 kPa. The black solid and dashed lines in Figure 12 show the pressure behavior during the injection and production stages of the 3rd FA-CSI with the spike representing the 3rd foam flood. Similar to previous FA-CSI cycles, the production volume, indicated by the red line in Figure 12, increased in the early stages of production, followed by a long plateau region. Incremental oil recoveries and the amount of produced oil were smaller compared to the previous FA-CSI cycles. ΔP across the sandpack initially increased and reached a constant value towards the end of the production stage. Figure 13 shows the foaming solution volume in the green line and pressure build-up across the sandpack in the black lines versus time during the injection of the third foam slug. Produced oil during the 3rd FA-CSI was 4.44 g and the incremental RF was 1 %OOIP. 3rd FA-CSI cycle was followed by final depletion at 50kPa/hr rate to reach the atmospheric condition.

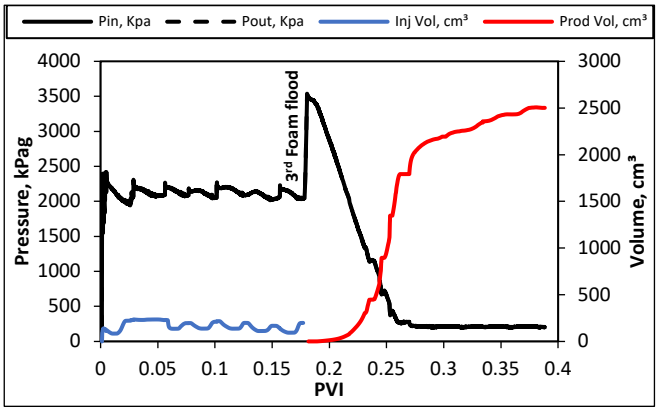

Fig. 12. Inlet and outlet pressures (kPag) and cumulative production and injection volumes (cm^3) during the 3rd FA-CSI

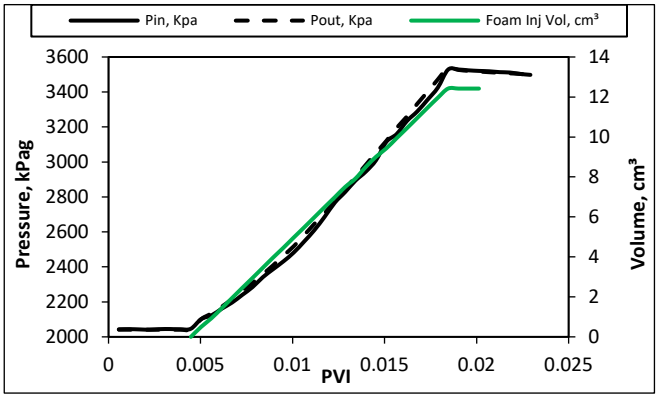

Fig. 13. Foaming solution volume (mL) and Pressure build-ups across the sandpack (kPag) during the 3rd foam flood

The incremental recovery data for all flooding tests conducted on sandpack number 2 are presented in Table 4 and plotted in Figure 14. During the primary depletion step, the recovery factor was 5.88 %OOIP. The 1st CSI cycle resulted in an RF of 13.75 %OOIP, followed by 6.76 %OOIP for the 2nd CSI cycle. The 3rd CSI cycle had the lowest RF among the three CSI cycles at 4.99 %OOIP. The incorporation of three FA-CSI cycles increased the RF by an additional 8.00 %OOIP.

Table 4. Incremental and cumulative recoveries for sandpack 2.

	Incremental oil, g	Cumulative oil, g	RF (%OOIP)
Primary depletion	26.10	26.10	5.88
1st CSI	9.98	36.08	8.13
	36.02	72.10	16.25
	15.03	87.13	19.64
2nd CSI	14.74	101.87	22.96
	8.40	110.27	24.85
	5.31	115.58	26.05
	1.57	117.15	26.40
3rd CSI	12.91	130.06	29.31
	7.44	137.50	30.99
	1.81	139.31	31.40
1st FA-CSI	9.55	148.86	33.55
	1.31	150.17	33.84
	0.68	150.85	33.99
2nd FA-CSI	17.56	168.41	37.95
	1.78	170.19	38.35
	0.25	170.44	38.41
3rd FA-CSI	3.33	173.76	39.16
	1.11	174.88	39.40

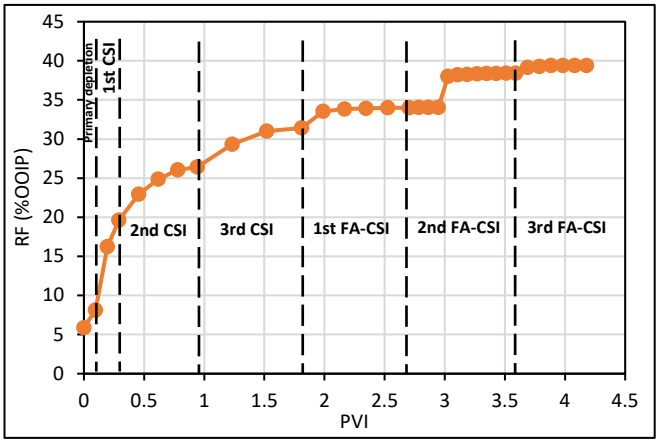

Fig. 14. Plot of oil recoveries in all the steps of the flooding experiments for sandpack number 2

3.7 Recovery factors

In this section, incremental recoveries for all eight sandpacks are presented. Recovery factors were calculated based on the mass of the produced oil divided by the mass of the original oil in place and are shown in Figure 15.

As depicted in Figure 15, recovery factors for the primary depletion stage were less than 6 %OOIP for all sandpacks. The 1st CSI had the highest recovery factor, ranging from 5% to 14 %OOIP, and the lowest volume of injected solvent among all the CSI cycles. This could be attributed to the availability of more oil in place during the 1st CSI cycle. Recovery factors for the 3rd CSI were small, ranging from 1% to 5% of OOIP in all eight sandpacks. The recovery factors increased by 10 to 14 %OOIP for FA-CSI cycles, as seen in Figure 15. The addition of foam as a slug to CSI after solvent injection, and then putting the system back under production, increased incremental recovery factors.

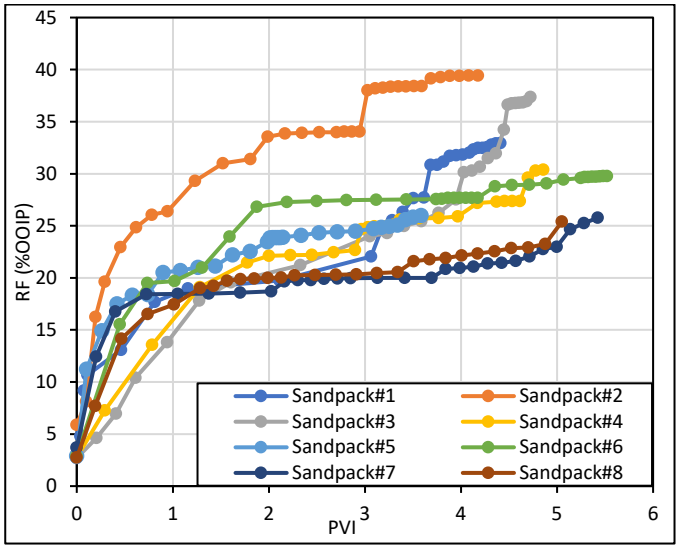

Fig. 15. Recovery factors (%OOIP) for all 8 sandpacks from primary depletion step to the end of the 3rd FA-CSI.

3.8 Foam performance during FA-CSI

This section compares foam performance in terms of pressure build-ups and recovery factors for different sandpacks. Recovery factors for the FA-CSI cycles ranged from 0.03% to 7% OOIP, as shown in Figure 16. For sandpacks 1 to 3, which had larger wormholes, pressure build-ups and recovery factors were higher. Conversely, for sandpacks 4 to 8, with smaller wormholes, recovery factors were higher during the later stages of foam floods. The reason for the higher recovery factors in sandpacks 1 to 3 was the presence of larger wormhole sizes, which provided a higher surface area to connect with the oil-saturated matrix inside the sandpack. Pressure build-ups during foam floods ranged from 10 kPa to 580 kPa, depending on the amount of solvent injected prior to the foam floods, the amount of injected foam, and the system pressure before the foam injection, as shown in Figure 17. For sandpacks 4 to 8 with smaller wormholes, higher pressure build-ups were observed in the later stages of the FA-CSI process, comparing the blue bars versus the red and green bars in Figure 17. Foam flood during the 3rd FA-CSI, represented by the blue bars, showed the highest flow resistance (ΔP) and recovery factors in sandpacks with smaller wormholes. For sandpacks 1 to 3 with larger wormholes, lower foam volumes were required during the later stages of foam floods. In contrast, for sandpacks 4 to 8 with smaller wormholes, higher foam volumes were required during the later stages of foam floods. A solvent flood followed by a foam flood (green bars) required lower foam volume and yielded higher recovery factors than a foam flood followed by a solvent flood. Recovery results showed that foams were more effective at blocking flow in earlier cycles. Despite this, the cumulative oil recovery factor was between 35 and 40 %OOIP and running CSI cycles with solvent and

foam led to addition of 8 to 14 %OOIP to oil recovery beyond what was achieved at the end of the 3rd CSI cycle with no foam.

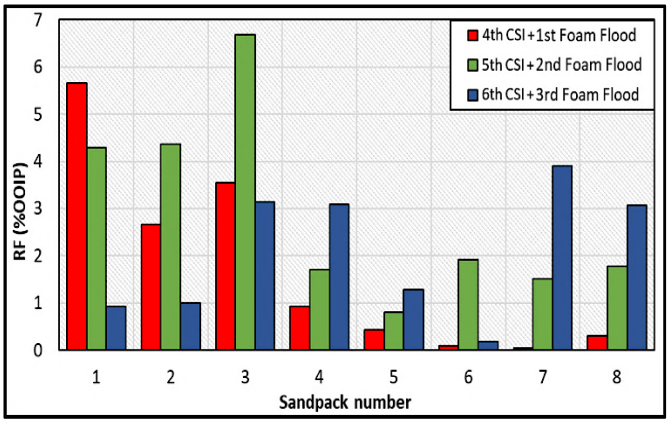

Fig. 16. Recovery factors (%OOIP) for all 8 sandpacks during FA-CSI floods.

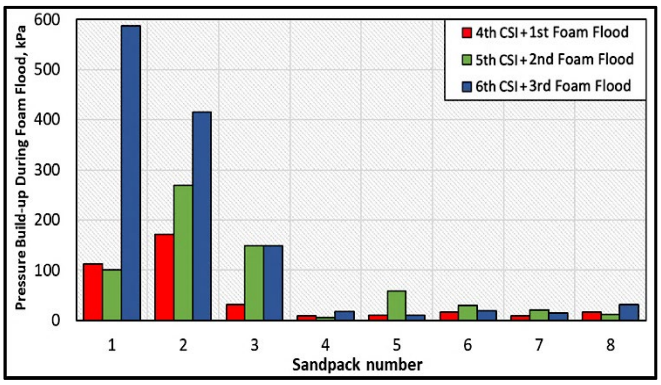

Fig. 17. Pressure build-ups (kPa) during foam floods for all 8 sandpacks.

3.9 Post-flood residual saturations

After the completion of the 3rd FA-CSI cycle, the systems were depressurized to ambient conditions and then opened. Dean-Stark measurements were taken as a function of length along the sandpacks. Table 5 and Figure 18 show the sampling locations for sandpack number 2. Four samples along the length of the sandpacks (30.5cm) were taken within the matrix, labeled as "M", and one sample consisted of the whole wormhole, labeled as "W". Dean-Stark is a material balance technique, and the outputs are mass of oil, water, and solids in each tested sample. Table 5 shows the oil percentage in each Dean-Stark sample.

The first observation that can be made by comparing the residual oil contents in different sections of the sandpack is that the values for the wormhole and matrix are very different. For the matrix, the saturation profiles show that $(\frac{\text{oil mass (gr)}}{\text{sample mass (gr)}}) \times 100$ was 14.49%, at the closed end, see Table 5. The oil content decreased until it reached 10.94% at the open end, the injection/production face, of sandpack number 2. Thus, there was oil displacement within the matrix from the closed end to the open end.

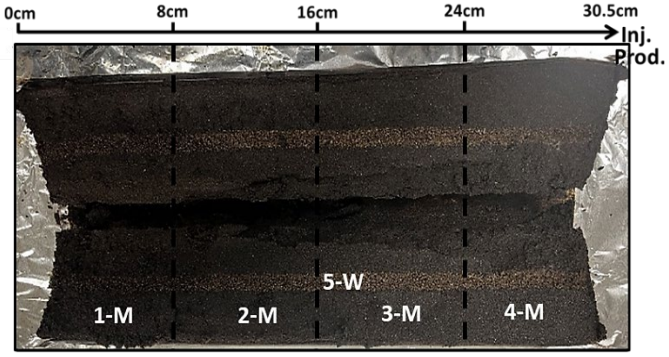

Fig. 18. Sampling locations along the length of sandpack#2.

Table 5. Dean-Stark measurements of residual oil content along the length of sandpack 2.

	Length interval, cm	Sample, g	Oil, g	Oil, %
1-M	0-8.0	567.48	82.21	**14.49**
2-M	8.0- 16.0	637.52	77.74	**12.19**
3-M	16.0-24.0	627.67	75.08	**11.96**
4-M	24.0-30.5	654.55	71.62	**10.94**
5-W	Wormhole	123.72	10.17	**8.22**

3.10 Gas storage

In this section, gas storage capacity during solvent floods for the first three CSI cycles is analyzed. Figure 19 shows the gas storage volumes for a CO_2 and propane solvent mixture during the 1st, 2nd, and 3rd CSI cycles. Stored gas volumes for each CSI cycle were calculated based on the injected and produced gas volumes (cm^3) at standard conditions (0°C and 1 atm). Stored gas volume increased with the number of CSI cycles as more empty pore space became available with increasing CSI cycles and higher cumulative oil production. However, no clear relationship between the wormhole size and gas storage capacity in the sandpacks was observed. It was determined that the stored gas volume was a function of the pore volume rather than the wormhole size, since the wormhole size is negligible compared to the reservoir. The gas mixture (30% C_3H_8 and 70% CO_2) can be stored inside the sandpacks in the form of dissolved gas in the oil or in saline aquifer connected to the reservoirs from the bottom or sequestered in depleted pore spaces. The pore volumes of the sandpacks averaged around $500cm^3$, as shown in Table 3.

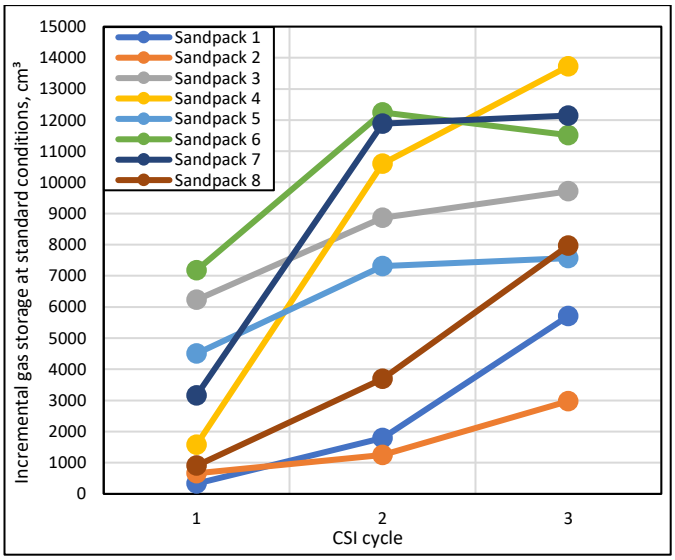

Fig. 19. Stored solvent mixture (CO_2 +C_3H_8) volumes during 1st, 2nd, and 3rd CSI cycles.

4 Discussion

This section provides a summary and comparison of results from all primary depletion, CSI, and FA-CSI experiments conducted in eight sandpacks with findings from existing literature. First, we compare the primary depletion and CSI cycles' performance in our tests with the results of works done by [25, 26, 27]. The performance of cyclic solvent injection depends on various factors such as solvent type, depletion rate, reservoir heterogeneity, gravity force, and initial oil saturation. Figure 20 shows the cumulative recoveries for primary pressure depletion and CSI experiments in eight sandpacks compared with the results from the literature. Differences in recovery factors between studies can be attributed to the above-mentioned variables. The black points in Figure 20 represent the recovery values generated during the current study, while the blue, red, and orange dots represent the results of experiments conducted by [25, 26, 27], respectively.

In a study conducted by [25], a 1 m long core with a 9 cm diameter was used for primary depletion and four CO_2 CSI cycles, see the blue dots in Figure 20. The core was positioned vertically, with a porosity of 39%, and permeability to brine was calculated to be 4.5 D. The core was saturated with live oil with a viscosity of 15000 mPa·s. Primary production at low rates (<10 kPa/hr) yielded an 11.5 %OOIP recovery. During CSI cycles 1 to 3, depletion rates remained at 50 kPa/hr, but the final 4th CSI cycle had a reduced depletion rate of 8 kPa/hr, resulting in a 5 %OOIP incremental recovery. CSI cycles 1 to 3 showed an incremental recovery of 6 %OOIP, 5.4 %OOIP, and 3.9 %OOIP, respectively. Recoveries achieved are within the range of the recoveries we measured for pressure depletion and three CSI cycles. Aside from the vertical core positioning and low depletion rates during primary recovery and the 4th CSI, the other parameters are similar to our experiments. The results from [25] indicate the effectiveness of oil pooling and gravity drainage on production, highlighting the impact of core orientation and low depletion rates on CSI performance. Foamy oil flow improved recovery under low depletion rates, resulting in 11.5 %OOIP and 5 %OOIP recoveries for primary depletion and 4th CSI cycle, respectively. Flipping the core vertically led to gas rising through the core, diluting oil with CO_2 solvent, and causing oil pooling at the bottom and higher gas saturation at the top of the sandpack.

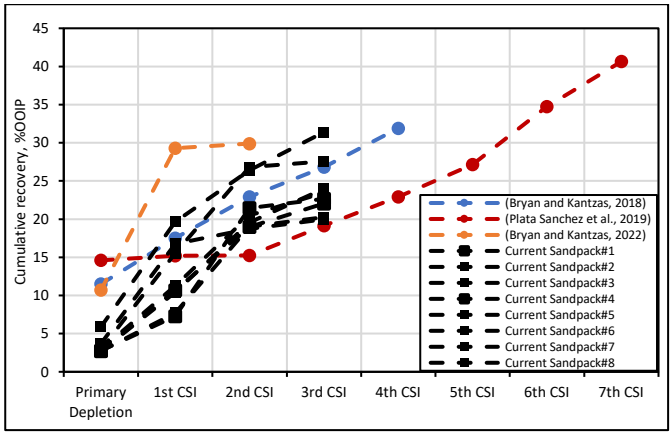

Fig. 20. Comparison of primary depletion and CSI experimental results in eight sandpacks with the literature

[26] conducted CSI tests on horizontal core, CSI cycles 1 and 2, and vertical core, CSI cycles 3 to 7, using solvent mixtures with 70% CH_4 and 30% C_3H_8 at varying depletion rates. In their study, core flood tests were undertaken to explore the impacts of gravity drainage, pressure depletion rate, solvent composition, and initial oil saturation on the recovery factor during the CSI process. Tests were conducted in a 37 cm sandpack with 38% porosity and 1.8 D permeability. The heavy oil used had a viscosity similar to that in both our study and the one conducted by [25]. To evaluate the effects of solvent mixture and core orientation on CSI, their experimental results, red dots in Figure 20, were compared with current and literature data. Comparing red dots to our current results, black datapoints, running primary production under similar conditions but in a vertical orientation, [26] achieved a 14.6 %OOIP recovery, significantly higher than the 3 to 5 %OOIP in our tests, showing the potential of foamy oil mechanisms in vertical cores for improved oil recovery within specific solution GOR and live oil viscosity ranges. Experimental work done by [26] highlighted that the oil recovery factor per CSI cycle was relatively consistent and repeatable over multiple cycles, in contrast to horizontal configurations, where production typically ceased after 2 to 3 CSI cycles. As shown, for CSI cycles 1 and 2, incremental recoveries were negligible, but recovery improved significantly when the core was flipped into the vertical position for CSI cycles 3 to 7, as seen by the red dots. [26] achieved a 40 %OOIP final recovery. A study by [27] revealed that the efficiency of the CSI decreased drastically after the 1st cycle, see the orange dots in Figure 20. The flooding procedure involved primary depletion, followed by 2 CO_2 CSI cycles. The initial pressure depletion stage resulted in an oil recovery of 10.7 %OOIP, while the first CSI cycle showed a significant incremental recovery of 18.6 %OOIP, reaching a cumulative recovery factor of 29 %OOIP

after just one cycle. Subsequent 2nd CSI cycle exhibited smaller incremental oil recovery, showing only a 0.6 %OOIP increment.

Lastly, we compare the FA-CSI cycles' performance in our tests with the works done by [27, 28, 29]. [27] conducted foam injection following primary depletion and 2 CSI cycles to enhance oil recovery in a horizontal core. They investigated the process of FA-CSI using the same oil, the same CSI solvent, saturation pressures, and depletion rates as in the study by [25]. However, the major difference was the inclusion of a glass bead on the top section of the sand in the horizontal flooding setup. The experiment was conducted in a heterogeneous core system with a diameter of 3 in. and a length of 30.5 cm, using foam consisting of 0.5 wt.% "SurEOR Foam 5000" surfactant and CO_2 gas. The system had a porosity of 36% and an absolute permeability of 20.5 D. The addition of glass beads increased the overall permeability and introduced a permeable channel at the top. [28] developed a methodology for foam-assisted cyclic steam injection in the core and [29] conducted four cycles of nitrogen foam-assisted CO_2 CSI in a sandpack using the surfactant and polymer combination, 0.3 wt.% SDS + 0.3 wt.% HPAM.

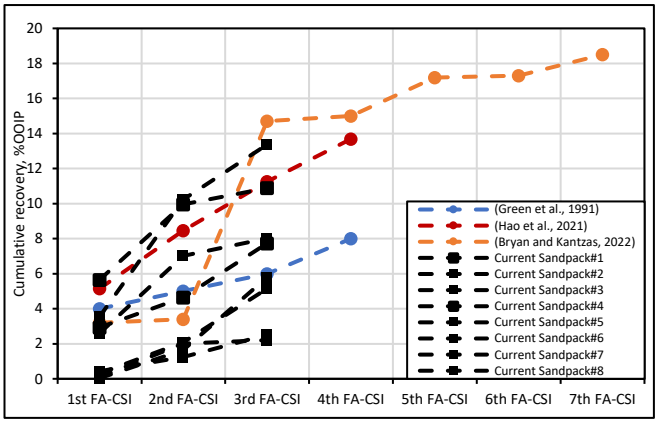

Fig. 21. Comparison of FA-CSI experimental results in eight sandpacks with the literature.

Figure 21 shows the results of the cumulative recoveries for FA-CSI cycles for our current work, black points, and work in the literature [27, 28, 29]. Our results fall within the recovery values reported in the literature, comparing the black points in Figure 21 with the blue, red, and orange dots. Foam injection successfully blocked flow and allowed for the regeneration of the initial CSI response. In the work by [27], 7 FA-CSI cycles increased the overall RF by 18 %OOIP, with the final RF being 47.8 %OOIP, see the orange dots in Figure 21. Similar to our observations, the effect of foam injection appeared to be short-lived in the heterogeneous system, as observed from the cumulative recovery during the later cycles. Subsequent low incremental RF for later FA-CSI cycles suggested the difficulty in blocking off the highly permeable sections. Our observations were consistent with the trends observed in the literature in terms of recoveries during CSI and FA-CSI cycles.

5 Conclusions

Sandpack injection experiments allowed us to draw the following conclusions: Compared with the CSI process, FA-CSI increased cumulative oil recovery and oil production rate. Adding inexpensive CNC foams as a slug to CSI after solvent injection and then putting the system back under production increased incremental oil recovery in wormhole-induced sandpacks by up to 14% OOIP. Cellulose nanocrystals are considered more cost-effective compared to other nanoparticles. The production costs for CNC are lower due to the abundant availability of cellulose from renewable sources like wood and agricultural by-products. CNC are estimated to be significantly cheaper than other nanoparticles such as carbon nanotubes or metal oxides, which involve more complex and expensive manufacturing processes. Instead of bringing modified CNC to the interface for stabilization, the synergism between DTAB and native CNC was exploited to obtain Pickering foams with high stability. Our results showed that foamy oil flow played a key role during production, with most of the oil production occurring in the section surrounding the wormhole. Additionally, the volume of injected foaming solution equaled 10% to 20% of the wormhole volume. Solvent injection followed by foam injection showed higher incremental oil recoveries and pressure build-ups than foam injection followed by solvent injection. The solvent mixture (CO_2 + C_3H_8) enhanced the CO_2-based CSI process. A higher mole fraction of C_3H_8 in the CO_2 stream in the solvent mixture resulted in a lower solvent injection volume and higher oil recovery. CSI performance, especially in later cycles, was better for sandpacks with bigger wormholes. During foam injection, pressure build-ups and oil recoveries were higher for sandpacks with bigger wormholes. Combining (CO_2 + C_3H_8)-CSI and Foam is a new process to improve cyclic solvent injection performance in heavy oil CHOPS reservoirs. Our laboratory experiments offer valuable performance data, enabling companies to make informed decisions regarding the viability and benefits of FA-CSI compared to traditional CO_2-based CSI. We have demonstrated that FA-CSI can lead to increased oil production and extended productive life in post-CHOPS reservoirs, especially those in the Lloydminster region. Additionally, the focus on environmentally friendly 'green' foam solutions aligns with industry trends towards sustainable practices for EOR operations.

The implementation of FA-CSI for EOR faces several limitations. Firstly, ensuring uniform foam propagation in heterogeneous reservoirs is challenging. The presence of wormholes in post-CHOPS reservoirs complicates foam distribution. Permeability reduction and formation damage after foam injection are other concerns. The high initial costs of FA-CSI development present financial obstacles. Foam stability over extended residence times inside the reservoir is critical for the success of FA-CSI in field applications. Exploring strategies for scaling up from laboratory to field operations requires pilot testing. Despite the promising potential of FA-CSI for EOR, addressing these challenges is crucial for field implementation.

References

1. D.M. Adams, J. Pet. Technol., **34**, 1643-1650, (1982).
2. M.B. Dusseault, InPETSOC Can. Int. Pet. Conf., PETSOC-2001, (2001).
3. G.A. Han, M.I. Bruno, M.B. Dusseault, J. Can. Pet. Technol., **46**(04), (2007).
4. Z. Du, F. Zeng, C. Chan, J. Energy Resour. Technol., **137**(4), 042901, (2015).
5. H. Ma, D. Huang, G. Yu, Y. She, Y. Gu, Energy & fuels, **31**(1), 418-28, (2017).
6. L. Lin, H. Ma, F. Zeng, Y. Gu, SPE Heavy Oil Conf. Can., 170098-MS, (2014).
7. M.R. Mworia, Z. Wu, K. Shu, S. Jiang, Q. Gou, Z. Chen, A.A. Said, Fuel, **361**, 130645, (2024).
8. M.A. Ahmadi, S. Zendehboudi, A. Bahadori, L. James, A. Lohi, A. Elkamel, I. Chatzis, Ind. Eng. Chem. Res., **53**(41), 16091-106, (2014).
9. A. Al Bahlani, Al Muatasim, T. Babadagli, SPE Annu. Tech. Conf. Exhib, 124047-MS, (2009).
10. F. Du, Diss. Faculty of Graduate Studies and Research, University of Regina, (2016).
11. J. Ivory, J. Chang, R. Coates, K. Forshner. J. Can, Pet. Technol., **49**(09), 22-33, (2010).
12. X. Sun, H. Zhao, Y. Zhang, Y. Liu, G. Chen, W. Wang, Fuel, **254**, 115656, (2019).
13. J. Ivory, J. Chang, R. Coates, K. Forshner, J. Can. Pet. Technol., **49**(09), 22-33, (2010).
14. A. Alshmakhy, B. Maini, SPE Heavy Oil Conf. Can., 157823-MS, (2012).
15. A.Q. Firouz, F. Torabi, SPE Heavy Oil Conf. Can., 157853-MS, (2012).
16. A.R. Shokri, T. Babadagli, J. Pet. Sci. Eng., **137**, 144-56, (2016).
17. H. Ma, G. Yu, Y. She, Y. Gu, J. Pet. Sci. Eng., **170**, 267-79, (2018).
18. X. Jia, F. Zeng, Y. Gu, SPE Heavy Oil Conf. Can., 170157-MS, (2014).
19. S.H. Talebian, R. Masoudi, I.M. Tan, P.L. Zitha, J. Pet. Sci. Eng., **120**, 202-215, (2014).
20. M.T. Janssen, A.S. Mutawa, R.M. Pilus, P.L. Zitha, Energy Fuels, **33**(6), 4951-4963, (2019).
21. K. Green, E. Isaacs, K.N.N. Chhom, J. Can. Pet. Technol., **30**, (1991).
22. S. Etemad, A. Kantzas, S. Bryant, J. Pet. Sci. Eng., **194**, 107540, (2020).
23. S. Etemad, A. Kantzas, S. Bryant, Fuel., **276** :118063, (2020).
24. S. Etemad, A. Telmadarreie, A. Kantzas, S. Bryant, Colloids Surf. A: Physicochem. Eng. Asp., **648**, 129274, (2022).
25. A. Kantzas, J. Bryan, Final Report Submitted to PTRC, PTRC No. HO-UC-01-17, (2018).
26. A.M. Plata Sanchez, Master's Thesis, Schulich School of Engineering, (2019).
27. A. Kantzas, J. Bryan, Final Report Submitted to PTRC, PTRC No. HO-PERM-01-2020, (2022).
28. K. Green, E. Isaacs, K.N. Chhom, J. Can. Pet. Technol., **30**(03), (1991).
29. H. Hao, J. Hou, F. Zhao, H. Huang, H. Liu, RSC Adv., **11**(2), 1134-1146, (2021).
30. P. Carlson, M. Campbell, A. Kantzas, Tech. Meeting/Pet. Conf. South Saskatchewan Sect., (1995).
31. G. Coskuner, K. Naderi, T. Babadagli, J. Pet. Sci. Eng., **133**, 475-82, (2015).
32. O. Ojumoola, H. Ma, Y. Gu, Energies, **13**(19), 5047, (2020).